High-efficiency photovoltaics based on semiconductor nanostructures
Award Number DE-FG36-08GO18016

Performing Organizations:	University of California, San Diego, University of Texas at Austin
Key Technical Contacts:	P. K. L. Yu, pyu@ucsd.edu, D. Wang, dwang@ece.ucsd.edu
	E. T. Yu, ety@ece.utexas.edu
DOE HQ Technology Manager:	Brian Hunter, 303.275.4934, brian.hunter@go.doe.gov
Project Monitor:	Michael Wofsey, 720-356-1367, michael.wofsey@go.doe.gov
Budget:	$883,568 (DOE), $225,000 (UCSD, UTA matching)
Personnel:	UCSD includes 2 faculty, 3 graduate students
	UT includes 1 faculty, 3 graduate students/postdoctoral researchers

Objectives

- Exploration of concepts for high-efficiency photovoltaics based on semiconductor quantum wells and nanowires
- Development of high-efficiency quantum-well and quantum-dot solar cells exploiting scattering effects from subwavelength metal and dielectric structures to engineer photon propagation paths within the photovoltaic device
- Development of high-efficiency photovoltaic devices based on semiconductor nanowire heterostructures
- Demonstration of basic concepts with the potential to enable realization of single pn-junction, quantum-well solar cells with power conversion efficiency approaching predicted theoretical limit (for unconcentrated sunlight) of ~45%

Accomplishments

- Demonstration of increased power conversion efficiency in GaInAsP/InP quantum-well solar cells compared to InP homojunction solar cells (~5-7% increase in power conversion efficiency)
- Demonstration of extended wavelength response in quantum well/quantum dot solar cells
- Demonstration of increased power conversion efficiency in quantum-well solar cells incorporating nanostructure scattering effects relative to quantum-well solar cells without nanostructured scatterers (~17% increase in power conversion efficiency)
- Development and demonstration of substrate removal process for fabrication of ultrathin solar cells incorporating light management approaches based on scattering from nanostructures
- Demonstration of photovoltaic power conversion in nanowire-based solar cells consisting of n-InAs nanowires on p-Si substrates.
- Demonstration of light trapping/light absorption enhancement in vertical Si nanowire array solar cells.
- Demonstration of photovoltaic power conversion in nanowire-based solar cells consisting of axial p/n Si nanowire arrays.
- Demonstration of photovoltaic power conversion in nanowire-based solar cells consisting of radial p/n Si nanowire arrays.
- Demonstration/simulation of the core doping effect to the photovoltaic power conversion in nanowire-based solar cells consisting of radial p/n Si nanowire arrays.
- Demonstration of the conformal electrode coating effect to the photovoltaic power conversion in nanowire-based solar cells consisting of radial p/n Si nanowire arrays.
- Demonstration of increased photovoltaic power conversion in nanowire-based solar cells consisting of radial p/n Si nanowire arrays by surface passivation (8% of total energy conversion efficiency).
- Demonstration of photovoltaic power conversion in nanowire-based photoelectrochemical cells (PECs) consisting of ZnO nanowire arrays on ITO, Si, etc. substrates.

- Demonstration of photovoltaic power conversion in nanowire-based PECs consisting of 3D ZnO/Si branched nanowire arrays on large-scale low cost solution etched Si substrates (IPCE >90% for 700-900nm, and overall hydrogen generation efficiency of 3% accomplished).
- Demonstration of high photovoltaic power conversion in nanowire-based PECs consisting of 3D ZnO/Si branched nanowire arrays on nanoimprinting patterned and RIE etched Si substrates.
- Demonstrated selective generation of hydrogen or oxygen from the 3D ZnO/Si branched nanowire array photoelectrodes by tailoring the doping in the Si nanowire cores.
- Demonstration of photovoltaic power conversion in nanowire-based PECs consisting of CuO and Cu_2O nanowire array electrodes.

Future Directions

- Optimization of metal/dielectric scattering structures for optical absorption enhancement in ultrathin quantum-well and quantum-dot solar cells.
- Further development of substrate removal and related fabrication processes.
- Characterization and optimization of carrier confinement effects in, and carrier escape from, quantum-well and quantum-dot structures.
- Fabrication and further improvement of semiconductor nanowire heterostructures for high-efficiency photovoltaic devices.
- Study of photovoltaic power conversion and stability in nanowire-based 3D TiO_2/Si branched nanowire array photoelectrodes.
- Study the ALD surface coating effect on the photovoltaic power conversion and stability in nanostructure photoelectrodes.

---

1. Introduction

The objective of this project was to exploit a variety of semiconductor nanostructures, specifically semiconductor quantum wells, quantum dots, and nanowires, to achieve high power conversion efficiency in photovoltaic devices. In a thin-film device geometry, the objectives were to design, fabricate, and characterize quantum-well and quantum-dot solar cells in which scattering from metallic and/or dielectric nanostructures was employed to direct incident photons into lateral, optically confined paths within a thin (~1-3um or less) device structure. Fundamental issues concerning non-equilibrium carrier escape from quantum-confined structures, removal of thin-film devices from an epitaxial growth substrate, and coherent light trapping in thin-film photovoltaic devices were investigated. In a nanowire device geometry, the initial objectives were to engineer vertical nanowire arrays to optimize optical confinement within the nanowires, and to extend this approach to core-shell heterostructures to achieve broad-spectrum absorption while maintaining high open-circuit voltages. Subsequent work extended this approach to include fabrication of nanowire photovoltaic structures on low-cost substrates.

2. Technical Approach

With regard to thin-film heterostructure device geometries, initial efforts focused on the design and demonstration of InP/InGaAsP quantum-well solar cells in which scattering by metal or dielectric nanoparticles would couple incident light into optical modes confined by the refractive index contrast between an InGaAsP multiple-quantum-well region and surrounding InP electrode layers. This would enable increases in optical absorption within multiple-quantum-well layers that were sufficiently thin that photogenerated carriers could escape efficiently to generate photocurrent. In subsequent work, efforts focused on the development of a substrate removal process that would enable fabrication of structures in which a thin (~0.5-3um) device structure would serve as a slab waveguide structure within which optical modes would be strongly confined. Incorporation of metal/dielectric sub-wavelength scattering structures on the bottom of such a device would enable scattering of long-wavelength photons, for which absorption efficiency can be low, into confined modes to increase absorption. The thin-

film geometry would allow such structures to be combined with antireflection coatings on the top of the device. The final device concept targeted in this work is shown schematically in Figure 1.

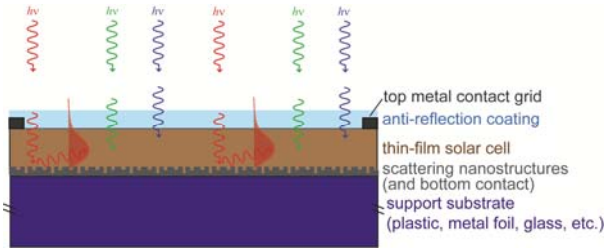

Figure 1. Schematic diagram of thin-film solar cell structure with epitaxial growth substrate removed and device transferred to alternate support substrate, metal/dielectric subwavelength structures integrated on the bottom of the device for coupling of long-wavelength photons into guided modes for increased absorption, and antireflection coating incorporated on top surface of device.

Regarding the nanowire photovoltaic devices, efforts have been focused on (i) vertical core-shell nanowire array solar cells and (ii) 3D branched nanowire photoelectrochemical cells. For the vertical nanowire solar cells, we have studied the metal mediated solution etching of Si nanowires and the ICP-RIE etched Si nanowires with nanoimprinting lithography (NIL) (Figure 2a). N-Si substrates with different background doping levels (n or n^+) were used based on simulation of the p/n junction depth and surface B diffusion. The nanowire solar cells were constructed in the following ways in order to study the charge separation/collection process: (a) nanowires are directly embedded in PDMS, tips exposed by RIE etching, and deposited with top contact of ITO or ITO/Ag grid; (b) nanowires are coated with conformal layer of ITO contact, embedded in PDMS, coated with ITO or ITO/Ag grid top contacts; (c) nanowires are coated with ALD Al_2O_3 passivation layer, embedded in PDMS, tips exposed by RIE etching, and deposited with top contact of ITO or ITO/Ag grid; etc. The comparison studies between (a), (b), and (c), while sometimes samples with different nanowire diameters and/or densities, allow us to isolate and understand the effects of light absorption (J_{sc}), charge separation pathway and collection and surface traps (V_{oc}), and fill factors (series resistance), etc. Similarly for photoelectrochemical cells (PECs), wet etched and RIE etched vertical Si nanowires (p-type and n-type) are used as backbone and ZnO nanowire branches are grown using solution hydrothermal method (Figure 2b). To better understand the 3D nanowire PEC photoelectrodes, we have compared both p-type or n-type core Si nanowires, p-Si or p^+-Si nanowires, ZnO nanowires directly on planar Si substrate, and ZnO seedling layer on Si substrates, etc. Figure 2b shows a typical cross section SEM image of 3D ZnO/Si nanowire arrays sample from solution etched Si nanowire and hydrothermal ZnO nanowire branches.

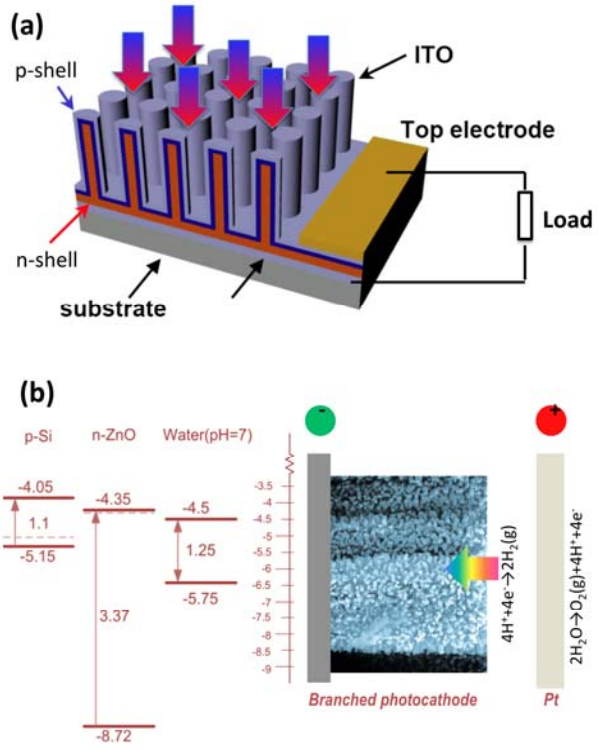

Figure 2. (a) The schematic illustration of the vertical nanowire array solar cells consists of the radial p/n junctions. In some cases, the substrate is the same n-type Si as the nanowire core; the top electrodes can are Ag grid on ITO coating with or without PDMS embedding layer. (b) The energy band diagram of the n-ZnO/p-Si branched nanowire photoelectrodes. The SEM image of a cross section version of the branched nanowires are shown. It was shown that the hydrogen are generated at the surface of ZnO nanowire branches while O_2 are generated from the counter electrodes (Pd).

3. Results and Accomplishments

For the portion of the program focused on thin-film heterostructure devices, the key results, referenced to project tasks, were as follows (Tasks 1, 3, 5, 7, 9. 11 were associated with this portion of the project):

- Demonstrated enhancement in long-wavelength photon absorption in quantum-well solar cells via scattering from metallic (Au) nanostructures on solar cell surface [Tasks 1, 3]
- Demonstrated improved power conversion efficiencies (~1.07x) in quantum-well solar cell compared to homojunction solar cell, and in quantum-well solar cell with nanostructured scatterers compared to same device without scatterers (~1.17x) [Tasks 5, 7]
- Fabrication and characterization of ultrathin quantum-well, quantum-dot, and reference solar cells with substrate removed and metal/dielectric scattering structure on back side of device [Tasks 9, 11]

In our initial work, InP/GaInAsP quantum-well and reference InP homojunction structures were designed and grown by metalorganic chemical vapor deposition, and solar cell devices were fabricated from these epitaxial layer structures. Current-voltage characterization of these devices demonstrated that power conversion efficiency was improved by ~1.05-1.07x in quantum-well devices relative to the InP homojunction solar cell. Incorporation of metal (Au) or dielectric nanostructures to scatter incident light into optical waveguide modes associated with the heterostructure yielded a further improvement of up to 1.17x in power conversion efficiency.

Subsequently, GaAs/InGaAs/InAs quantum dot and quantum dot-in-well epitaxial layer structures were grown by molecular-beam epitaxy through a collaboration initiated with researchers at the NASA Jet Propulsion Laboratory, and devices were fabricated and characterized in efforts to achieve further extensions in long-wavelength response (beyond those possible in simple quantum-well structures). These experiments resulted in the demonstration of photocurrent response in a GaAs-based solar cell extending past 1000nm, well beyond the GaAs band edge at ~850nm.

The most recent work in this area has been carried out via a collaboration between project researchers at UT Austin and a group at the University of Karlsruhe in Germany. This work was directed towards realization of thin-film quantum-well and quantum-dot solar cell structures in which the device layers were removed from the epitaxial growth substrate to enable realization of the concept illustrated in Figure 1. Specifically, epitaxial layer structures were grown in which an AlGaAs sacrificial etch-stop layer was incorporated beneath the actual device layers, as shown in Figure . The figure shows the device structure for a GaAs p-i-n junction reference device. Similar structures have been grown, and fabricated into devices, with quantum-well and quantum-dot structures incorporated into the i-layer shown in the figure.

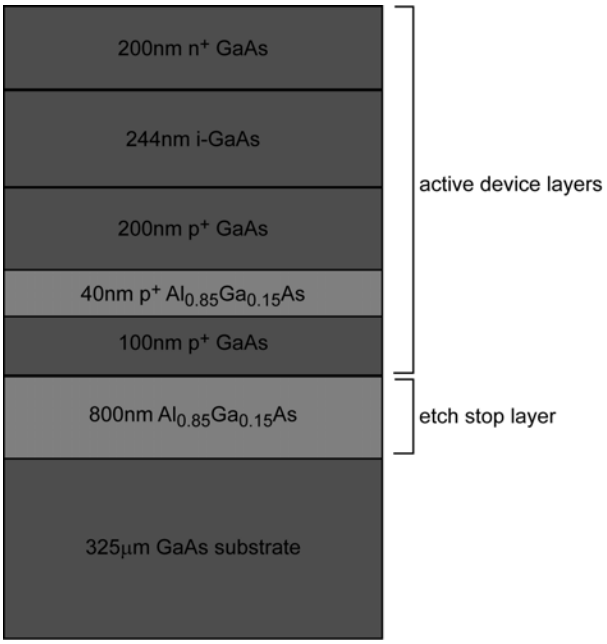

Figure 3. Schematic diagram of epitaxial layer structure for p-i-n solar cell device with AlGaAs etch stop layer to facilitate separation of the active device layers from the growth substrate. The structure shown is for a reference GaAs p-i-n structure. Analogous structures in which InGaAs/InAs quantum wells and quantum dots have been incorporated into the i-layer have also been grown and fabricated into devices.

Following epitaxial growth, metallization layers were evaporated onto the top (as-grown) surface and the surface of an alternate support substrate. The resulting metal surfaces were then bonded together and the growth substrate removed by a combination of mechanical polishing and chemical etch processes. We have also, very recently, implemented an epitaxial liftoff process that allows the device layers to be separated from the growth substrate while preserving the substrate for subsequent re-use. Figure shows a schematic diagram and scanning electron micrograph of a GaAs/InGaAs quantum-well solar cell device structure ~750nm in thickness separated from its epitaxial growth substrate and bonded to an alternate support structure, in this case a Si wafer. We have verified the functionality of these devices in both current-voltage measurements and photocurrent response spectroscopy. Figure (5)

shows current-voltage characteristics for a representative device following the substrate removal processing, and Figure (6) shows photocurrent response spectra for a GaAs reference device, GaAs/InGaAs quantum-well solar cell device, and GaAs/InGaAs/InAs quantum-well/dot solar cell device. As expected, photocurrent response at successively longer wavelengths is observed for the reference, quantum-well, and quantum-well/dot devices.

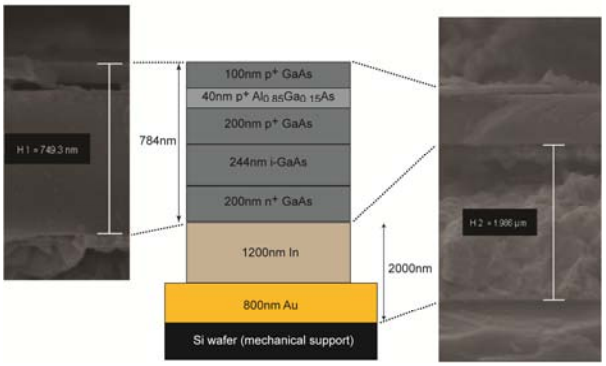

Figure 4. Schematic diagram of device structure (except for top metal contact) following separation of device layers from epitaxial growth substrate and transfer to alternate mechanical support structure (Si wafer). Also shown are cross-sectional SEMs confirming that the device layers were successfully transferred and bonded to the mechanical support.

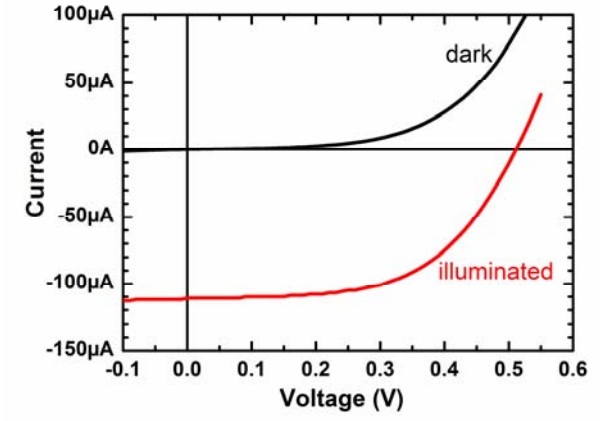

Figure 5. Current-voltage characteristics for GaAs-based solar cell device following substrate removal process, in the dark and under illumination.

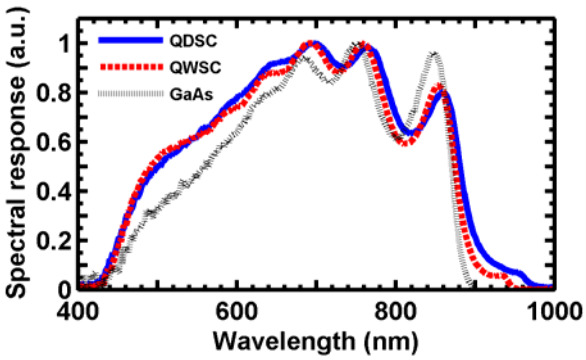

Figure 6. Normalized spectral response of thin-film devices after substrate removal process: (gray, hashed) p-i-n GaAs; (red, dashed) GaAs/InGaAs quantum-well solar cell; and (blue, solid) GaAs/InGaAs/InAs quantum-well/dot solar cell.

We have performed detailed numerical simulations and modeling of structures in which metal and dielectric sub-wavelength structures are incorporated below the active device layers in an device that has been removed from its epitaxial growth substrate, as illustrated schematically in Figure 1. The structure that was studied numerically, and optimized structural parameters obtained via a genetic algorithm, is shown in Figure . A detailed model for quantum-well optical absorption, incorporating appropriate polarization-dependent selection rules for heavy hole-conduction band and light hole-conduction band transitions, and quantum-mechanical calculations of confined-state envelope functions, was developed and applied, and compared to results obtained for a simpler, bulk-like model for quantum-well optical absorption. The resulting ratio of absorption with the grating structure shown in Figure relative to that for a structure with a planar metal rear contact, as a function of wavelength, is shown in Figure . At shorter wavelengths, Fabry-Perot oscillations due to interference in the thin-film device structure are visible. At longer wavelengths, large increases in absorption are seen at particular wavelengths, corresponding to the combination of absorption peaks in the quantum-well and coupling to specific optical modes within the thin-film structure. Calculations employing bulk-like absorption characteristics in the quantum well differ from those for the quantum-mechanical treatment due to incorporation of polarization-dependent selection rules in the latter approach. Experimental verification of these behaviors was underway at the conclusion of this program.

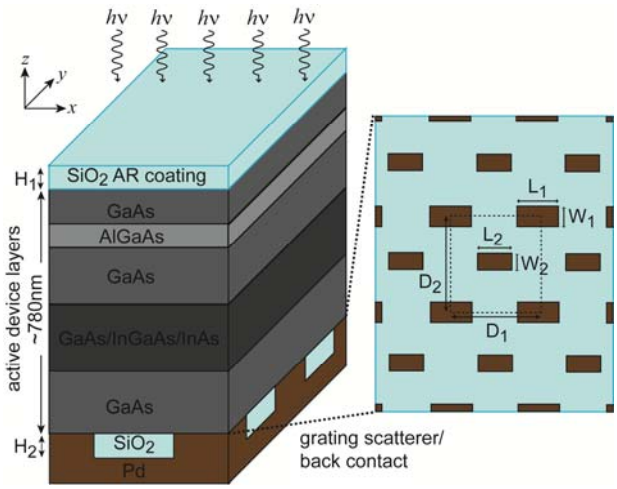

Figure 7. Diagram of the device structure employed in numerical simulations, with a broadband, two-dimensional grating located on its rear with dimensions W_1 = 336 nm, L_1 = 474 nm, W_2 = 92 nm, L_2 = 356 nm, D_1 = 900 nm, D_2 = 1130 nm. These specific dimensions were obtained via optimization using a genetic algorithm.

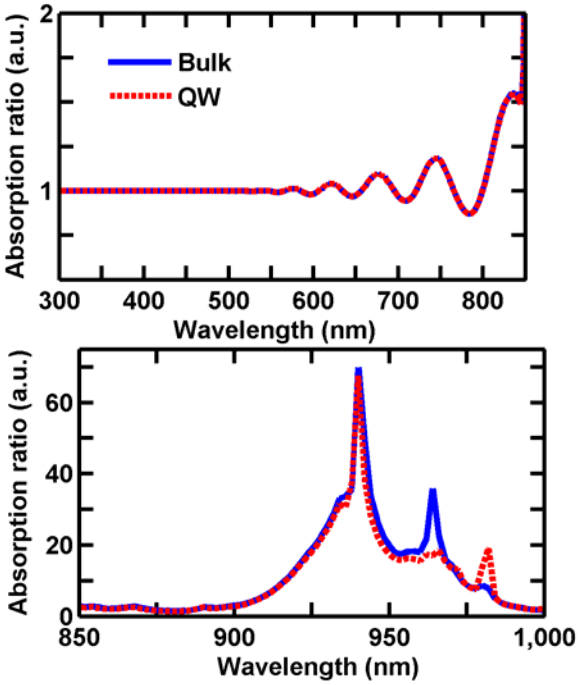

Figure 8. Spectral dependence of the ratio of absorption of incident radiation by a quantum-well solar cell with Pd/SiO_2 nanostructured backside scattering elements relative to the same device with a planar backside layer of Pd. The ratio is shown for calculations using bulk InGaAs material permittivity (blue, solid line) and using quantum-mechanical absorption calculations (red, dashed line).

For Tasks 2, 4, 6, 8, 10, 12 of the program that focused on nanowire devices, the major results, were as follows:

- Demonstration of photovoltaic power conversion in nanowire-based solar cells consisting of n-InAs nanowires on p-Si substrates. [Tasks 6, 8]
- Demonstration of light trapping/light absorption enhancement in vertical Si nanowire array solar cells. [Tasks 2, 6, 8]
- Demonstration of photovoltaic power conversion in nanowire-based solar cells consisting of axial p/n Si nanowire arrays. [Tasks 4, 6, 8]
- Demonstration of photovoltaic power conversion in nanowire-based solar cells consisting of radial p/n Si nanowire arrays. [Tasks 6, 8]
- Demonstration/simulation of the core doping effect to the photovoltaic power conversion in nanowire-based solar cells consisting of radial p/n Si nanowire arrays. [Tasks 6, 8]
- Demonstration of the conformal electrode coating effect to the photovoltaic power conversion in nanowire-based solar cells consisting of radial p/n Si nanowire arrays. [Tasks 6, 8]
- Demonstration of increased photovoltaic power conversion in nanowire-based solar cells consisting of radial p/n Si nanowire arrays by surface passivation (8% of total energy conversion efficiency). [Tasks 6, 8]
- Demonstration of photovoltaic power conversion in nanowire-based photoelectrochemical cells (PECs) consisting of ZnO nanowire arrays on ITO, Si, etc. substrates. [Tasks 10, 12]
- Demonstration of photovoltaic power conversion in nanowire-based photoelectrochemical cells consisting of 3D ZnO/Si branched nanowire arrays on large-scale low cost solution etched Si substrates (IPCE >90% for 700-900nm, and overall hydrogen generation efficiency of 3% accomplished). [Tasks 10, 12]
- Demonstration of high photovoltaic power conversion in nanowire-based PECs consisting of 3D ZnO/Si branched nanowire arrays on nanoimprinting patterned and RIE etched Si substrates. [Tasks 6, 8]
- Demonstrated selective generation of hydrogen or oxygen from the 3D ZnO/Si branched nanowire array photoelectrodes by tailoring the doping in the Si nanowire cores. [Tasks 10, 12]
- Demonstration of photovoltaic power conversion in nanowire-based PECs consisting of CuO and Cu_2O nanowire array electrodes. [Tasks 10, 12]

For the nanowire photovoltaic research, we have studied the direct integration of vertical III/V nanowire array on Si substrate and fabrication of photovoltaic devices. (Figure 9). The devices show very good photoresponse in a very broad wavelength range (350nm – 3μm) and the solar energy conversion efficiency of 1.1% at room temperature and 2.5% at 110K under 1.5AM sun illustration. Core/shell heterostructure nanowires were successfully grown, but no device were studied.

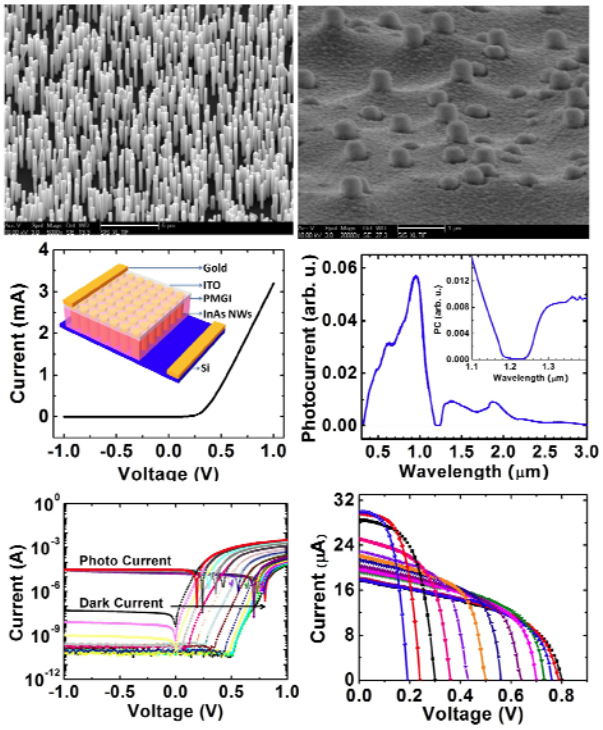

Figure 9. InAs nanowire on Si substrate nanowire solar cells. Vertical nanowire arrays were growth without metal catalyst in MOCVD on p-Si substrate. InAs nanoiwre were embedded in PDMS and consequently coated of top ITO contact after RIE etching and exposure of InAs nanowire tips, Both V_{oc} and J_{sc} change with temperature.

In order to better understand the working principles in nanowire solar cells, we took Si radial p/n junction as a model system. 1D Poisson simulation revealed that high doping level is necessary to create radial p/n junctions. Figure 10 shows the simulation results and the corresponding doping conditions to create effective radial p/n junctions. Different surface passivation coatings were studied, including PECVD SiN_x and ALD Al_2O_3 coatings; ITO was coated using sputtering as both passivation and conformal electrode to nanowires were studied;

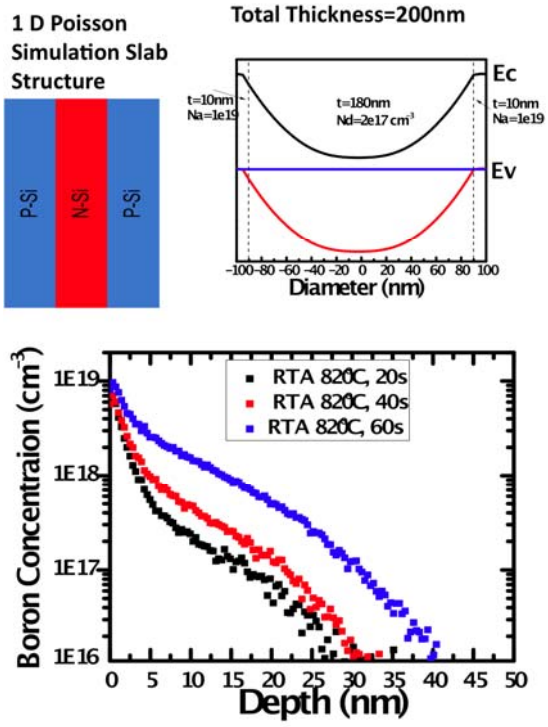

Figure 10. 1D Poisson simulation and the junction depth, along with the SIMS doping profile.

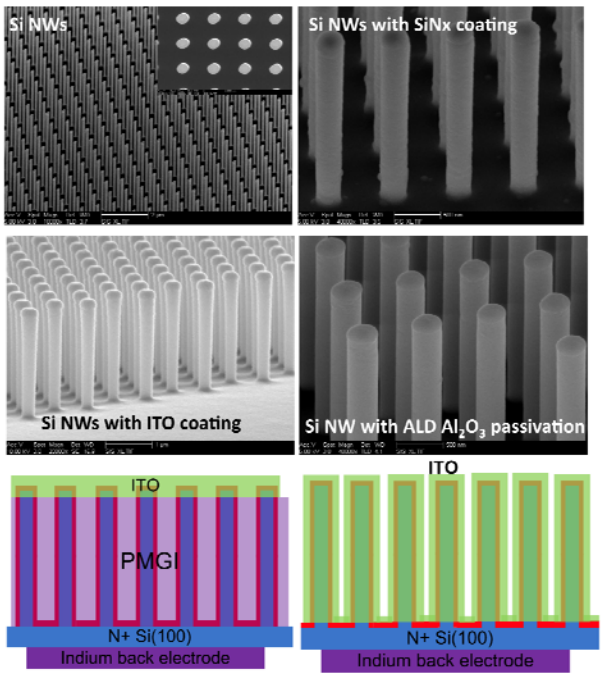

Figure 11. ICP-RIE etched vertical Si nanowires with radial p/n junction and different surface passivation coating, such as PECVD SiNx, Sputtered ITO, and ALD Al_2O_3. The devices are fabricated by with or without the PMGI embedding. Top contacts are ITO or ITO/Ag grid.

different annealing conditions were also studied. Table 1 summarized the device performance of the Si radial junction nanowires, one can clearly see (i) SiN_x surface passivation improved the solar cell efficiency by about 250%, (ii) conformal ITO contact reduces the series resistance significantly and improve the energy conversion efficiency about 5 times compared to bare Si p/n junction solar cells and about 2.3 times to that of SiN_x passivated devices, (iii) optimized doping profile and the junction depth control is critical for the efficiency (two step annealing of dopants at 800°C almost tripled the solar cells efficiency), (iv) The use of Ag mesh grid on ITO top contact significantly reduce the series resistance and increase of efficiency, (v) high quality ALD coated Al_2O_3 passivation gives the best results of 8% energy conversion efficiency with the short circuit current density is comparable to previous result, while the open circuit voltage, fill factor and efficiency are greatly improved (Figure 12).

Table 1. Summary of Si nanowire solar cells.

Device area	passivation	Doping	Ag grid contact	V_{oc} (V)	J_{sc} (mA/cm^2)	FF	PCE (%)	Rs (ohm)
area~0.45 cm^2	NO	820°C 20s	200nm	0.13	5.52	0.27	0.216	50.05
area~0.21 cm^2	SiNx	820°C 20s	200nm	0.15	12.15	0.269	0.54	58.28
area~0.45 cm^2	SiNx	820°C 60s	200nm	0.145	10.1	0.27	0.421	21.54
area~0.72 cm^2	ITO	820°C 20s	No	0.22	4.65	0.255	0.261	58.58
			200nm	0.235	13.37	0.285	1.05	30.20
area~0.624 cm^2	ITO	800°C 10s ; 800°C 3hr.	200nm	0.314	26.56	0.296	2.80	20.85

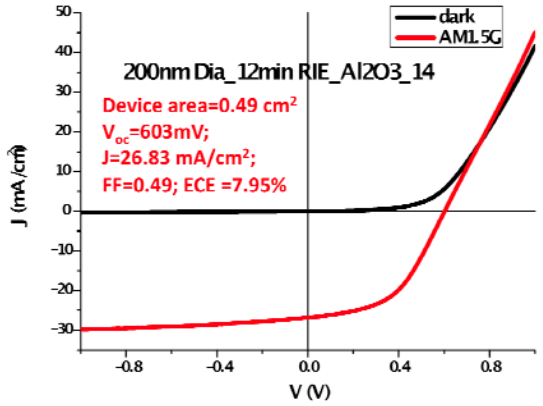

Figure 12. Photovoltaic curve of Si radial nanowire solar cells with ALD Al_2O_3 passivation.

Separate effort on the nanowire photovoltaic devices, such as photoelectrochemical cells (PECs) were studied using nanowire and nanowire heterostructure photoelectrodes. First of all, the vertical nanowire arrays show enhanced light absorption due to the light trapping (black surface of Si nanowires of ZnO/Si nanowire arrays Figure 13). Secondly, the 3D nanowires show much enhanced photocurrent densities compared to the Si nanowire arrays (very unstable), ZnO nanowires on planar Si (identical doping to the nanowires), ZnO seeding layer coated on Planar Si, ZnO nanowire array on ITO, and bare Planar Si, etc. photoelectrodes. Very fast hydrogen evolution was observed. The 3D ZnO/Si branched nanowires also show very high incident photon – to-current efficiency (IPCE) (Figure 14). The nanowire heterostructure photoelectrodes show not only high IPCE (>90% at 700-900nm), but also response to very broad spectra (370nm to >1100nm). The comparison to the devices of ZnO nanowire on Si (very low (<2% for 400 – 950nm) and ZnO nanowires on ITO glass (only response to UV).

Studies were also performed on the ICP-RIE etched Si nanowires with well defined diameters defined by NIL. Specific focus was on the doping of the Si nanowire cores (trunks). Figure 15 shows the SEM images of the NIL/RIE Si nanowires with ZnO seeding layer and ZnO nanowire branched. We fabricated 3D branched nanowire heterostructures, consisting of vertical Si nanowire cores and uniform ZnO nanowire branches, to apply as PEC photoelectrodes. By tuning the doping in the p-type Si nanowire core, the photoelectrochemical H_2/O_2 generation can be

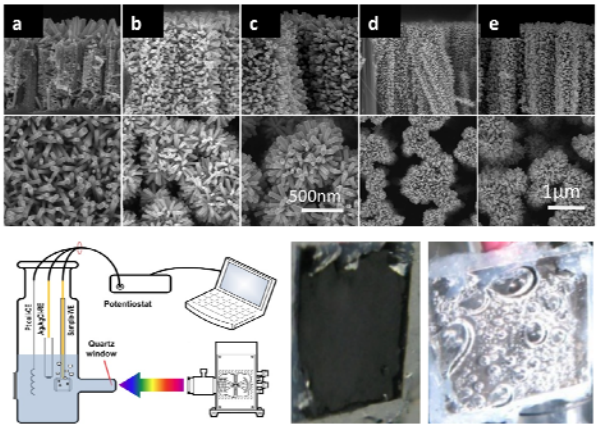

Figure 13. Cross-sectional view (top row) and top view (bottom row) SEM images of ZnO/Si branched NW arrays with different backbone and branch lengths. ZnO NW branches from growth for 2.5 hr on Si NWs with different lengths by chemical etching for (a) 5 min, (b) 10 min, and (c) 15 min, respectively (scale bar = 500 nm). ZnO NW branches grown for different time of (d) 30 min and (e) 2.5 hr on Si NW arrays etched for 15 min (scale bar = 1 μm). The PEC measurement setup and optical images of the surface of nanowire photoelectrode with or without light illustration. The

dark surface also indicated the enhanced light absorption due to light trapping effect.

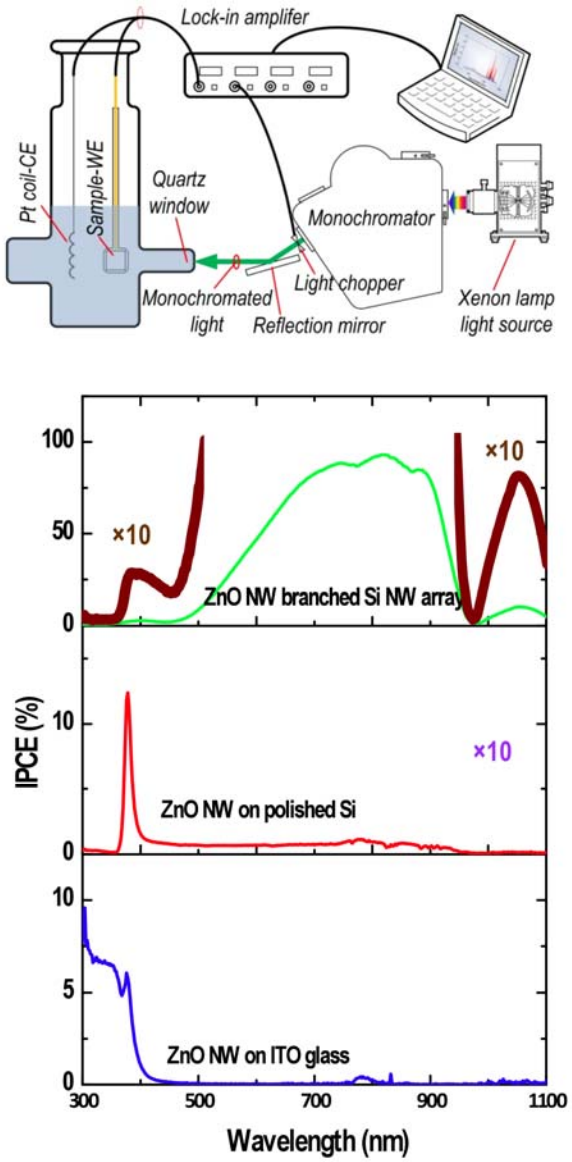

Figure 14. Incident photon conversion efficiency (IPCE) vs wavelength measurement and comparison between 2D ZnO/Si photoelectrodes to AnO nanowires on planar Si substrate, and pure ZnO nanowires on ITO glass.

adjusted. When the core is lightly doped, the p-Si/n-ZnO branched nanowire array electrodes provide photocathodic H_2 production with a broadband absorption from UV to near IR region, while the p^+-Si/n-ZnO branched NW arrays show photoanodic O_2 generation with photoresponse only to UV light. The photocurrents of these unique 3D n-ZnO/Si branched NW heterostructures are orders of magnitudes higher than that of the bare Si NW photoelectrodes.

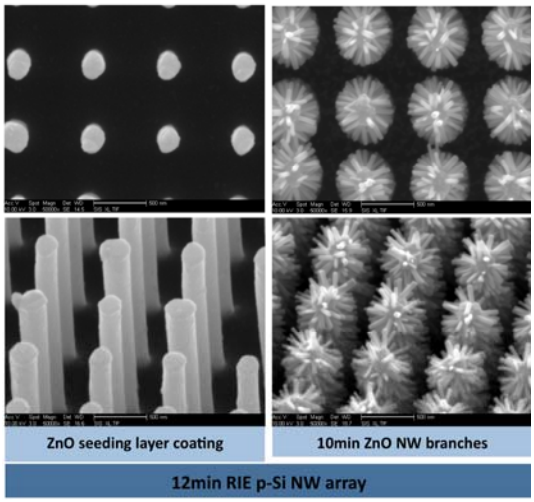

Figure 15. SEM images of NIL/RIE Si nanowires with ZnO seeding layer (coated by sputtering) and ZnO branches by hydrothermal growth.

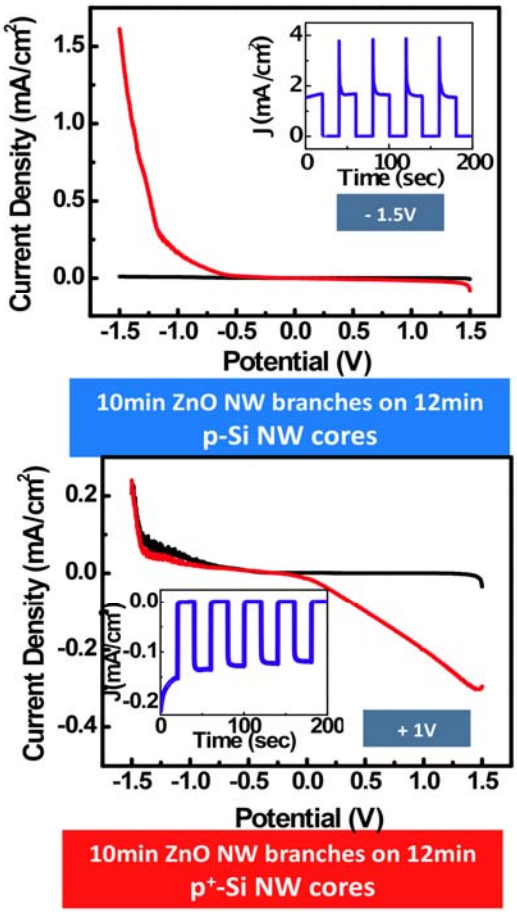

Figure 16. I-V characteristics of p-Si/n-ZnO (Si(100), p-Si, boron doped, resistivity of 1-20 Ωcm) and p^+-Si/n-ZnO (p^+-Si, boron doped,

resistivity of 0.001-0.004 Ωcm) branched nanowire photoelectrodes.

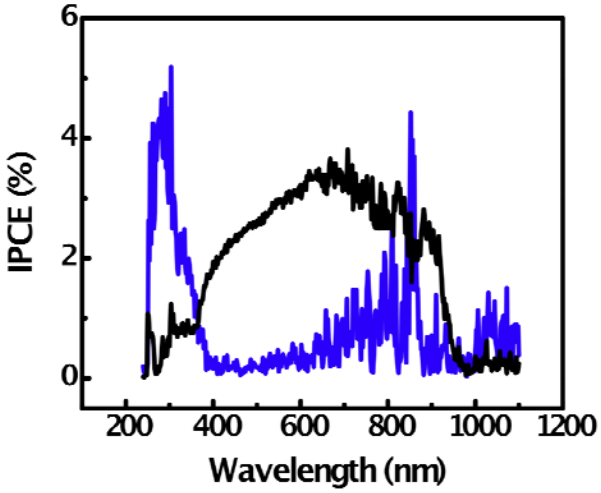

Figure 17. IPCE of NIL/RIE Si/ZnO branched nanowire photoelectrodes. p-Si/ZnO branched nanowires present a broad photo-response from UV to near IR region, while p^+-Si/ZnO branched NWs lead to photoresponse only to UV light.

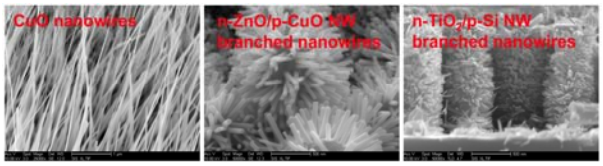

Figure 18. Future works on other nanowire PEC devices consists of CuO nanowires, 3D branched ZnO/CuO, and TiO_2/Si branched nanowrie photoelectrodes for high efficiency of better stability.

These unique 3D branched NW heterostructures are promising photoelectrodes for high efficient photoelectrochemical H_2 generation. A detailed study has been done to show the NW dimensions effect on the PEC performances and consequently optimize the heterostructure for optimum high efficient photoelectrochemical production of H_2.

Lastly, we have also carried out the PEC studies on new materials, including p-type CuO nanowires, and 3D branched ZnO/CuO, and TiO2/Si branched nanowries, which can lead to future studies for new photoelectrodes with high efficiency or improved corrosion resistivity and life time.

4. Special Recognitions, Awards, and Patents

In 2009 E. Yu was appointed to the Judson S. Swearingen Regents Chair in Engineering at the University of Texas at Austin. Research conducted under this program was the subject of invited talks by E. Yu, D. Wang, and P. Yu at many workshops and international conferences, as follows:

E. T. Yu, D. Derkacs, S. H. Lim, P. Matheu, D. M. Schaadt, W. V. Chen, and P. K. L. Yu, "Plasmonic nanoparticle scattering for enhanced performance of photovoltaic and photodetector devices," presentation at 2008 SPIE Optics+Photonics Conference, San Diego, CA, August 2008.

E. T. Yu, D. Derkacs, W. V. Chen, and P. K. L. Yu, "Quantum well and plasmonic nanostructures for high-efficiency photovoltaics," presentation at 2008 SPIE Optics+Photonics Conference, San Diego, CA, August 2008.

E. T. Yu, D. Derkacs, W. V. Chen, and P. K. L. Yu, "Plasmonic scattering enhancement of quantum-well solar cells," presentation at 2008 OSA Frontiers in Optics Conference, Rochester, NY, October 2008.

E. T. Yu, "Exploiting nanowires and nanoparticles for photovoltaics," presentation at Workshop on Research Frontiers and Capability Gaps for Controlling and Designing Functional Materials, Los Alamos, NM, January 2009.

E. T. Yu, "New technologies for solar energy harvesting: current reality and future potential," presentation at La Jolla Research and Innovation Summit, La Jolla, CA, April 2009.

E. T. Yu, "Plasmonic and nanoparticle scattering effects in high-efficiency photovoltaics," presentation at 2009 International Workshop on Physics of Semiconductor Devices, Delhi, India, December 2009.

D. Wang, "Synthesis of III-V Nanowires using MOCVD and Application for Photovoltaics", Department of Printed Electronics Engineering, Sunchon National university, Suncheon, Korea. February 2009. *(Invited)*

D. Wang, "Novel solar cells based on heteroepitaxial III/V semconductor nanowires arrays on silicon", NSTI – Nanotech/Greentech conference, Huston, TX, May 4, 2009.

D. Wang, "Synthesis of III-V Nanowires using MOCVD and Application for Photovoltaics", SCNU-WCU (Sunchon National university – World Class University) workshop, Suncheon, Korea. July 2009.

D. Wang, "Rational synthesis of semiconductor nanowires and application in electronics and optoelectronics", GI-NST conference, Mopko, Korea, November 5th, 2009.

D. Wang "Photovoltaics – Principles, Printed, and Printable", Master class (tutorial), ICPFE, Jeju, Korea, November 11th, 2009.

D. Wang, "Nanowires for optoelectronics and renewable energy," International Conference on One-dimensional Nanomaterials (ICON), Georgia Institute of Technology, Atlanta, GA. December 7-9, 2009.

E. T. Yu, "Engineering of plasmonic effects in photodetectors and high-efficiency photovoltaics," presentation at 2010 IEEE International Nanoelectronics Conference, Hong Kong, China, January 2010.

D. Wang, "Semiconductor Nanowire and High Sensitivity Photodetectors," *5th SINO-US Nano Forum,* Suzhou, China, May 5-7, 2010.

D. Wang, "Semiconductor Nanowire Photo-detectors," *6th Annual SF-BA Nanotech Council,* May 19, 2010.

D. Wang, "Semiconductor Nanowire Photo-voltaics," *Applications for Photovoltaic Systems* - Knowledge Foundation Webcast, June 10, 2010.

D. Wang, "Vertical Semiconductor Nanowire Photovoltaics", SPIE – Nano Solar Energy symposium, San Diego, CA, USA, Aug. 5, 2010.

D. Wang, "Nanowire photosensor and photo-voltaics", IEEE-nano/Nano Korea conference – Research Frontiers, KINTEX, Seoul, Korea, August 24-26, 2010.

P. K. L. Yu, B. Washom, D. Wang, E. T. Yu, "A Green Campus and PV Research", IEEE Solar Technology Workshop Austin, Texas, U.S.A., Sept. 16, 2010.

D. Wang, "Nanowires for Photodetectors and Photovoltaics", Nanowires10 (NW10) - *Physics and Applications of Physics and Applications of Semiconducting Nanowires Semiconducting Nanowires",* Foundation for Research and Technology, (FORTH) Heraklion, Crete (Greece), September 27-October 1, 2010,

D. Wang, "Nanowire materials and devices for optoelectronics, renewable energy, and medicines – research and commercialization", Saigon HiTech Park, Vietnam, Nov. 5, 2010.

D. Wang, P. Yu, "Nanowire Based Devices for Photosensing and Photovoltaics", OIDA annual meeting, Washington D. C., Nov. 16-18, 2010. (Poster Presentation)

D. Wang, "3D Branched Nanowire Heterojunction Photoelectrodes for High-Efficiency Solar Water Splitting and H_2 production", 2010 Workshop on Innovative Devices and Systems (WINDS), which will be held on the Big Island of Hawaii, December 5-10, 2010.

E. T. Yu, "Exploiting plasmonic and nanostructure-based scattering effects for photovoltaic devices," presentation at Lawrence Workshop on Epitaxy, Tempe, AZ, February 2011.

E. T. Yu, C. O. McPheeters, and P. C. Li, "Exploiting interactions among metal, dielectric, and semiconductor nanostructures for photovoltaic devices," presentation at 2011 Villa Conference on Interaction Among Nanostructures, Las Vegas, NV, April 2011.

E. T. Yu, C. O. McPheeters, D. Derkacs, and S. H. Lim, "Exploiting Nanostructure-based Scattering Effects in High-efficiency Photovoltaic Devices," presentation at 2011 Spring Meeting of the Materials Research Society, San Francisco, CA, April 2011.

D. Wang, "Nanowire and Oxide Materials for Optoelectronic and Photovoltaic Applications", First Sino-Korea Printed Electronics Workshop - Design, Synthesis, and Printing of Functional Organic and Inorganic Materials", Sunchon National University, Suncheon, South Korea, January 17, 2011.

D. Wang, "Semiconductor Nanowire Photovoltaics and Lighting Devices," International Conference on Materials and Advanced Technology (ICMAT), Suntec city, Singapore, June 26th to July 1st, 2011.

K. Sun, A. Kargar, Y. Zhou, K. Madsen, J. Yi, and D. Wang, "3D Branched Nanowire Photo-electrodes for High Efficiency Solar Water Splitting and Hydrogen Production", IMAPS/ACerS 7th International Conference and Exhibition on Ceramic Interconnect and Ceramic Microsystems Technologies (CICMT 2011), San Diego CA, 2011. (Best student paper award)

P. K. L. Yu, E. T. Yu, D. Wang, "Advances in semiconductor nanostructures for photonic applications", 20th International Symposium on Processing and Fabrication in Advanced Materials (PFAM XX), Hong Kong, December 2011.

5. Major Publications

The following archival journal articles explicitly acknowledging support from this program were published or have been accepted for publication:

D. Derkacs, W. V. Chen, P. M. Matheu, S. H. Lim, P. K. L. Yu, and E. T. Yu, "Nanoparticle-induced light scattering for improved performance of quantum-well solar cells," *Appl. Phys. Lett.* **93**, 091107 (2008).

C. O. McPheeters, C. J. Hill, S. H. Lim, D. Derkacs, D. Z. Ting, and E. T. Yu, “Improved performance of In(Ga)As/GaAs quantum dot solar cells via light scattering by nanoparticles,” *J. Appl. Phys.* **106**, 056101 (2009).

D. Hu, C. O. McPheeters, E. T. Yu, and D. M. Schaadt, “Improvement of performance of InAs quantum dot solar cell by inserting thin AlAs layers,” *Nanoscale Res. Lett.* **6**, 83 (2011).

E. T. Yu and J. van de Lagemaat, “Photon management for photovoltaics,” *MRS Bulletin* **36**, 424 (2011).

C. O. McPheeters, D. Z. Hu, D. M. Schaadt, and E. T. Yu, “Semiconductor heterostructures and optimization of light-trapping structures for efficient thin-film solar cells,” accepted for publication in *J. Opt.* (2012).

W. Wei, X.Bao, C. Soci, Y. Ding, Z. Wang, and D. Wang, “Direct heteroepitaxy of vertical InAs nanowires on Si substrates for broad band photovoltaics and photodetection,” *Nano Lett.* **9**, 2926 (2009).

K. Sun, Y. Jing, N. Park, C. Li, Y. Bando, and D. Wang, “Solution Process of Large Scale High Sensitivity ZnO/Si Hierarchical Nano-heterostructure Photodetectors”, Journal of American Chemical Society, 132, 15465 (2011).

K. Sun, W. Wei, Y. Jing, Yong Ding, Zhong Lin Wang, and D. Wang, “Crystalline ZnO Thin Film by Hydrothermal Growth”, ChemCommun, 47, 7776 (2011).

K. Sun, Y. Jing, C. Li, X. Zhang, R. Aguinaldo, A. Kargar, K. Madsen, K. Banu, Y. Zhou, Y. Bando, Z. Liu, D. Wang, "3D Branched Nanowire Heterojunction Photoelectrodes for High-Efficiency Solar Water Splitting and H2 Generation" Nano Letters, under revision, 2011.

7. University and Industry Partners

Research under this program was conducted at the University of California, San Diego and the University of Texas at Austin. Collaborations with NASA Jet Propulsion Laboratory and the University of Karlsruhe were undertaken for this project.